



Jurnal Teknologi Reaktor Nuklir

Tri Dasa Mega

Journal homepage: jurnal.batan.go.id/index.php/tridam

Synthesis and Characterization of Cesium Silicate to Determine Its Detailed Properties as Chemisorbed onto Structural Materials of Light Water Reactor During Severe Accident Conditions

I Wayan Ngarayana*

Research Center for Nuclear Reactor Technology, Research Organization for Nuclear Energy, National Research and Innovation Agency, BJ Habibie Integrated Science Area Building No. 80 Serpong, Tangerang Selatan 15312, Indonesia.

ARTICLE INFO

Article history:

Received: 02 February 2023

Received in revised form: 06 March 2023

Accepted: 07 March 2023

Keywords:

Cesium silicates

Source terms

Chemisorption

Retention

Synthesis

Crystal structure

ABSTRACT

Cesium chemisorption phenomenon strongly contributes to the source terms transport during light water nuclear reactor accidents. Large amounts of cesium silicates are identified to be chemisorbed onto structure material, reduce cesium volatility, and affect the late release and re-vaporization phenomena. Although it has been studied for a long time, several characteristics of these compounds are still under discussion. In this study, Cs_2SiO_3 , $\text{Cs}_2\text{Si}_2\text{O}_5$, and $\text{Cs}_2\text{Si}_4\text{O}_9$ were synthesized through the solid-state method and the results have been confirmed using X-Ray Diffraction (XRD) measurement. Furthermore, their crystal structures have been refined based on the XRD analysis. The crystal structure refinement of these compounds proves the previous studies, but with minor distinctions in the lattice parameters. XRD patterns changing over time when measured in the open-air environment also show that $\text{Cs}_2\text{Si}_4\text{O}_9$ is the most stable species among other cesium silicate species. This indicates that the chemisorbed Cs-Si-O compound onto the structural material as identified by previous studies is most likely $\text{Cs}_2\text{Si}_4\text{O}_9$ rather than Cs_2SiO_3 or $\text{Cs}_2\text{Si}_2\text{O}_5$. Therefore, detailed $\text{Cs}_2\text{Si}_4\text{O}_9$ identification including its thermodynamic properties characterization could be very useful to enhance the database that is being built to improve current source terms transport codes.

© 2023 Tri Dasa Mega. All rights reserved.

1. INTRODUCTION*

Source terms transport evaluation is an important part of Nuclear Power Plant (NPP) safety measurement, both during normal operation, accident scenarios, as well as decommissioning preparation [1]. Several codes had been developed to predict source terms inventory and their transport behavior [2-6]. However, most of the currently available codes are overestimated and could not

catch several physical events, i.e., late-release phenomena due to the chemisorption [7].

The chemisorption phenomenon is well-understood contributing significantly to the source terms release characteristic [8-10]. Source terms have a high possibility to react chemically either with structural materials and/or with other source terms to form certain compounds. These compounds can increase volatility so making them easier to be released out of the system or vice versa becomes less

*Corresponding author. Tel./Fax.: +6281804369643

E-mail: iway018@brin.go.id

DOI: 10.55981/tdm.2023.6803

volatile and accumulate inside of the structure. The silica contained in a number of structural materials together with oxygen has been known to have a significant impact on the cesium chemisorption phenomenon which is one of the biggest contributors to radiation exposure [11]. Although had been intensively studied, however, several aspects of cesium silicate (Cs-Si-O) are still under discussion [10, 12]. The aim of this study is to validate and improve understanding of Cs-Si-O compounds to support better database construction for more precise source term transport modeling. This study is conducted by synthesizing the most predicted stable chemisorbed Cs-Si-O compounds onto stainless steel structural material [8, 9, 13, 14], particularly Cs_2SiO_3 , $\text{Cs}_2\text{Si}_2\text{O}_5$ and $\text{Cs}_2\text{Si}_4\text{O}_9$.

2. METHODOLOGY

2.1. Specimen treatment

2.1.1. Received materials

Cesium carbonate (Cs_2CO_3) and silicon oxide (SiO_2) with 99.9% purities were provided by Nilaco Corp. Both Cs_2CO_3 and SiO_2 precursors were identified as stable compounds which have $P12_1/c1$ and $I\bar{4}2d$ space group, respectively.

2.1.2. Synthesis and preparation

Several techniques for synthesizing cesium silicate have been developed. Osaka et al., synthesize $\text{Cs}_2\text{Si}_2\text{O}_5$ and $\text{Cs}_2\text{Si}_4\text{O}_9$ using the solid-state method by mixing Cs_2CO_3 and SiO_2 with an atomic ratio of Si/Cs = 1.9 in the platinum crucible inside glovebox with moisture less than 1 ppm, adding a few ml of H_2O and dried at 50 °C, mixing residual powder using agate mortar then pressed into a green pellet at 200 MPa, and finally heated at 850 °C for 2 hours in a muffle furnace [11]. Similar to Osaka, Di Lemma synthesized $\text{Cs}_2\text{Si}_2\text{O}_5$ and $\text{Cs}_2\text{Si}_4\text{O}_9$ by exactly the same method except for the drying temperature that was kept at 150 °C and duration of heating treatment for around 8 and 4 hours, respectively [15]. Jeon synthesized Cs_2SiO_3 by mixing Cs_2CO_3 and SiO_2 with atomic ratio Cs/Si = 2 using a tubular mixer for 30 minutes, heated at 630 °C for 5 hours, heated at 800 °C for 3 days and heated again at 1050 °C for 18 hours [16]. Meanwhile, Minami and Kaneko synthesized $\text{Cs}_2\text{Si}_2\text{O}_5$ by melting Cs_2O and SiO_2 in a Pt crucible at 1350 °C for 1 hour and slowly cooled at the rate of 0.1 °C per minute [17, 18].

However, due to a lack of detail in the process, this experiment was unable to replicate the above methods. Nonetheless, cesium silicates have been

successfully synthesized in the following manner. Cs_2SiO_3 , $\text{Cs}_2\text{Si}_2\text{O}_5$, and $\text{Cs}_2\text{Si}_4\text{O}_9$ were synthesized using the solid-state method by mixing high-purity Cs_2CO_3 and SiO_2 with Cs/Si atomic ratios about 0.5, 1.0, and 2.0, respectively. The mixing process has been done on the ceramic mortar inside a glove box filled with argon gas to reduce contamination. A few amounts of distillate water were added as a solvent and then stirred for around 2 minutes to increase the solution's homogeneity. The solution was then dried for 3 hours at 150 °C inside a muffle furnace to remove the solvent. The solid solution was then pressed into a pellet before being heated slightly above the melting point of Cs_2CO_3 at 610 °C. Cs_2CO_3 is expected to decompose into Cs_2O and release CO_2 during this step. In the high-density pelleted environment, Cs_2O is supposed to react with SiO_2 then forming Cs_2SiO_3 , $\text{Cs}_2\text{Si}_2\text{O}_5$, or $\text{Cs}_2\text{Si}_4\text{O}_9$, depending on the Cs/Si atomic ratio of the solution. Although the expected compounds have been formed up to this point, they are still in the amorphous phase and thus cannot be observed using XRD. Because of that, to increase the crystallinity, the specimens were crushed, re-pelleted, and heated again at the temperature between 800-900 °C for 3 days. To avoid the influence of humidity, the entire heating process was done using a muffle furnace on the air atmosphere but was kept in airtight conditions shortly after the heating process ended.

2.2. Characterization

Table 1 shows the detail settings for the MiniFlex Rigaku XRD machine used for the characterization.

Table 1. MiniFlex Rigaku XRD machine parameters configuration.

Parameters	values
Voltage & current	40 kV, 15 mA
Goniometer	MiniFlex 300/600
Filter	None
Detector	D/teX
Scan mode	Continuous
Scan speed	10.0000 deg/min
Step width	0.0200 deg
Scan axis	Theta/2-Theta
Scan range	15.0000-80.0000 deg
Incident slit	1.250 deg
Length limiting slit	10.0 mm

The qualitative and quantitative analyses were carried out with the help of Rigaku embedded software PDXL2 and High Score Plus 3.05, which was equipped with the International Centre for Diffraction Data (ICDD) and Pearson's Crystal database.

3. RESULTS AND DISCUSSION

3.1. Cs_2SiO_3

Cs_2SiO_3 is a hygroscopic compound that makes synthesis and analysis extremely difficult. The sample's contact with open air was minimized by cooling down and preparing the sample for XRD processes inside the glove box filled with argon gas. Unfortunately, because the special airtight sample holder was not available, contact with air could not be avoided during the XRD measurement. However, by taking measurements as quickly as possible, the results should be still valid, particularly at low measurement angles.

As shown in Fig. 1, most XRD peaks match with ICDD 00-019-0318 as well as the previous experimental study by Jeon [16], indicating the formation of Cs_2SiO_3 . However, other strong unrelated peaks also exist. These unrelated peaks were identified as surface water due to the humidity absorption during measurement which was performed in an open-air environment.

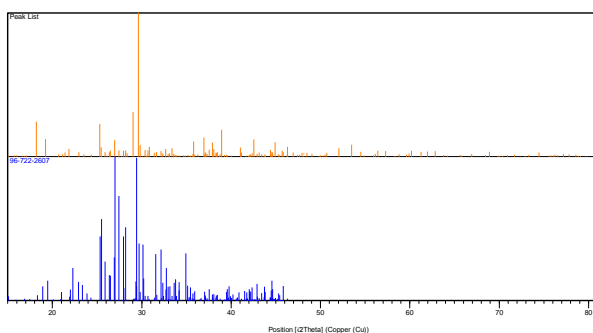


Fig. 1. XRD analysis of Cs_2SiO_3 specimen matches with International Centre for Diffraction Data (ICDD) 00-019-0318. However, some strong peaks, particularly at 18.2° , 26.0° , and 29.1° are related to surface water indicating its hygroscopicity.

Table 2. Lattice parameters of Cs_2SiO_3

Cell Parameters	Pearson's Crystal Data	This experiment
Space group	$P12_1/c1$ (14)	$P12_1/c1$ (14)
a (Å)	6.847	6.873
b (Å)	13.757	14.123
c (Å)	17.036	17.28
α	90.00°	90.00°
β	108.23°	110.98°
γ	90.00°	90.00°
V (Å ³)	1524.1	1567
Software	Bruker AXS CCD	PDLX2

The Cs_2SiO_3 crystal structure refinement was conducted using embedded software of Rigaku XRD machine and using Pearson's Crystal Data with entry

number 109590. As shown in Table 2, acquired cell parameter in this experimental study is relatively similar with the Pearson's Crystal Data. Furthermore, crystal structure of Cs_2SiO_3 as identified in this study is visualized in Fig. 2.

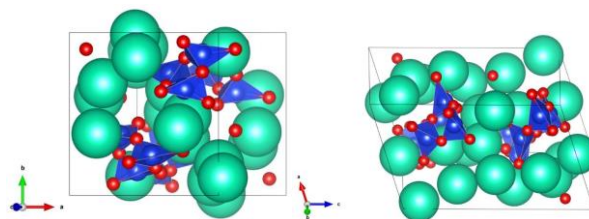


Fig. 2. Visualization of Cs_2SiO_3 crystal structure.

3.2. $\text{Cs}_2\text{Si}_2\text{O}_5$

As shown in Fig. 3, most measured peaks from the specimen are matched with ICDD card number 00-028-0336 indicating the $\text{Cs}_2\text{Si}_2\text{O}_5$ compound. Small peaks shifting exhibit parameter differences between measurement and ICDD reference. However, as shown in Fig. 4, XRD measurements using the same specimen in open air environment that was performed every 15 minutes reveal peak changing. Peak changing in this $\text{Cs}_2\text{Si}_2\text{O}_5$ specimen is correlated with humidity absorption, just like in Cs_2SiO_3 .

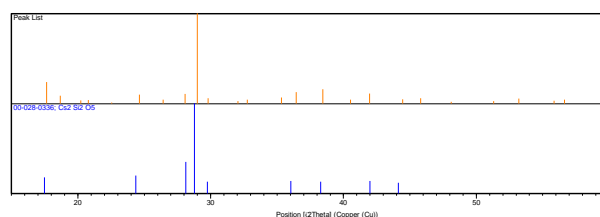


Fig 3. Measured peaks compared with ICDD card number 00-028-0336 indicate most of the structures are related to $\text{Cs}_2\text{Si}_2\text{O}_5$.

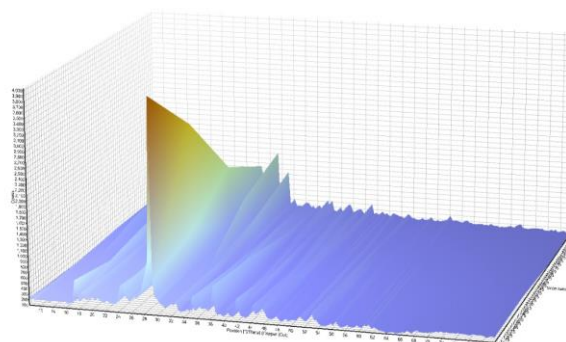


Fig. 4. XRD peaks changing of $\text{Cs}_2\text{Si}_2\text{O}_5$ specimen in line with the time when measured in the open-air environment exhibit hygroscopicity of this compound.

Since the ICDD card number 00-028-0336's crystallographic parameters are unavailable, the refinement was carried out using Pearson's Crystal

database under entry number 1921318. Table 3 shows that there is only a very slight deviation between the results of this experiment and the earlier studies. Based on the experimental result, then the schematic representation of $\text{Cs}_2\text{Si}_2\text{O}_5$ crystal structure finally also can be drawn as schematically shown in Fig. 5.

Table 3. Comparison of $\text{Cs}_2\text{Si}_2\text{O}_5$ crystallographic parameters

Cell Parameters	Pearson's Crystal Data	(F. Miradji, et al. 2020)	This experiment
Space group	$P12_1/c1$ (14)	$P12_1/c1$ (14)	$P12_1/c1$ (14)
a (Å)	10.061	10.206	10.180541
b (Å)	8.609	8.839	8.711289
c (Å)	18.414	18.720	18.632788
α	90.00°	90.00°	90.00°
β	122.76°	122.76°	122.76°
γ	90.00°	90.00°	90.00°
V (Å ³)	1341.2	-	1389.627669
Software	Enraf-Nonius CAD4T	DFT	PDLX2

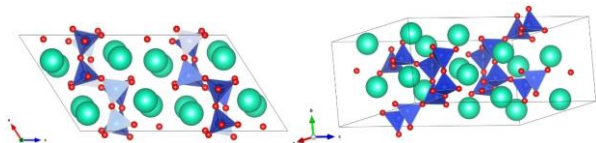


Fig. 5. Schematic representation of $\text{Cs}_2\text{Si}_2\text{O}_5$ crystal structure.

3.3. $\text{Cs}_2\text{Si}_4\text{O}_9$

The successful synthesis of the $\text{Cs}_2\text{Si}_4\text{O}_9$ specimen, as shown in Fig. 6, was verified by comparing the XRD reading with the ICDD card number 00-019-0318. However, there are at least two things to keep in mind. Aside from being dominated by $\text{Cs}_2\text{Si}_4\text{O}_9$, there are still small-intensity SiO_2 -related peaks that have a strong correlation with ICDD card number 01-085-0504. Although the profiles are exceptionally similar, there are shifting peaks in the experimental results when compared to the reference. This shifting occurs because of internal stress due to some factors, i.e., measurement environments, which affects crystal structure transformation. However, unlike Cs_2SiO_3 and $\text{Cs}_2\text{Si}_2\text{O}_5$, specimen of $\text{Cs}_2\text{Si}_4\text{O}_9$ is extremely stable and non-hygroscopic. This has been proven by the absence of a shift in the XRD peak even though it is measured repeatedly over a long period of time. Relatively stable $\text{Cs}_2\text{Si}_4\text{O}_9$ compound compared with Cs_2SiO_3 and $\text{Cs}_2\text{Si}_2\text{O}_5$ can be understood from their crystal structures as illustrated in Figs. 2, 5, and 7. Crystal structure of $\text{Cs}_2\text{Si}_4\text{O}_9$ consists of less

cesium atom and relatively well surrounded by covalent bonds constructed by silicon and oxygen atoms.

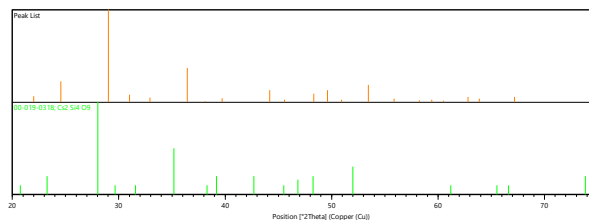


Fig. 6. Measured peaks from synthesized $\text{Cs}_2\text{Si}_4\text{O}_9$ specimen compared with ICDD card number 00-019-0318.

Suzuki et al., have measured low heat capacity of $\text{Cs}_2\text{Si}_4\text{O}_9$ using Physical Property Measurement System instrument [19]. Furthermore, Miradji, et al also tried to predict $\text{Cs}_2\text{Si}_4\text{O}_9$ crystal lattice parameters using density-functional theory (DFT) calculations [12]. Although the standard reference for peak list of this compound has been published by ICDD, its standard crystallographic parameters have not yet been established.

Based on the XRD measurement in Fig. 5, the indexation and lattice parameters refinement have been performed using PDLX2. By using $\text{Na}_2\text{Ti}_4\text{O}_9$ as prototype structure, this method generated several candidates with its crystallographic parameters. Crystal structure of this $\text{Cs}_2\text{Si}_4\text{O}_9$ was then constructed using VESTA code. As shown in Table 4, the result of this experiment is matching with the $P3c1$ space group that has been predicted by [12]. However, the final crystal lattice parameters of this experimental study are slightly different.

Table 4. Crystallographic parameters of $\text{Cs}_2\text{Si}_4\text{O}_9$ from the previous study compared with this experiment.

Cell Parameters	(F. Miradji, et al. 2020)	Experiment Result
Space group	$P3c1$	$P3c1$
a (Å)	12.180	9.409
b (Å)	12.180	9.409
c (Å)	9.703	9.491
α	90.00°	90.00°
β	90.00°	90.00°
γ	120.00°	120.00°
V (Å ³)	-	727.8
Software	DFT calculation ((initial prototype from $\text{K}_2\text{Ge}_4\text{O}_9$))	PDLX2

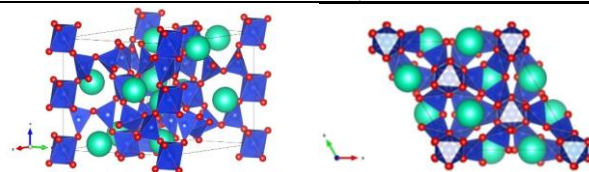


Fig. 7. Schematic representation of $\text{Cs}_2\text{Si}_4\text{O}_9$ crystal structure

4. CONCLUSION

The synthesis and crystal refinement of Cs_2SiO_3 , $\text{Cs}_2\text{Si}_2\text{O}_5$, and $\text{Cs}_2\text{Si}_4\text{O}_9$, as part of source terms studies, have been done successfully using a solid-state reaction. $\text{Cs}_2\text{Si}_4\text{O}_9$ is relatively stable compared with $\text{Cs}_2\text{Si}_2\text{O}_5$ and Cs_2SiO_3 . Both $\text{Cs}_2\text{Si}_2\text{O}_5$ and Cs_2SiO_3 easily absorb humidity when in an open-air environment. This hygroscopic property causes several issues during the synthesis and measurement processes. Despite the limited apparatus, the best measurement and refinement were performed using the Rigaku XRD machine's embedded software. $\text{Cs}_2\text{Si}_4\text{O}_9$ was refined based on $\text{Na}_2\text{Ti}_4\text{O}_9$ as a prototype and ICDD pattern number 00-019-0318, while $\text{Cs}_2\text{Si}_2\text{O}_5$ and Cs_2SiO_3 have been refined based on Pearson's Crystal Data number 1921318 and 109590 respectively. According to the restructured schematic crystal representations, Cs_2SiO_3 and $\text{Cs}_2\text{Si}_2\text{O}_5$ have more cesium atoms and are not well surrounded by covalent bonds constructed by silicon and oxygen atoms, making them unstable, especially in humid conditions. Therefore, of the three Cs-Si-O species, it is most likely that the compound that has been found to be chemisorbed in previous studies on the oxide layer of stainless steel should be $\text{Cs}_2\text{Si}_4\text{O}_9$. Consequently, further characterization of $\text{Cs}_2\text{Si}_4\text{O}_9$ needs to be done to complete the thermodynamic properties database that is being built.

ACKNOWLEDGMENT

This article is written based on data obtained by the author while conducting research at Nagaoka University of Technology. Therefore, the author is grateful to Analysis and Instrumentation Center (AIC), Nagaoka University of Technology who provided a part of experimental apparatus. Many thanks also to Professor Kenta Murakami from Tokyo University, Dr. Thi-Mai-Dung Do from Nagaoka University of Technology, Dr. Nhut Luu Vu from JAEA, and Professor Gordon from ANSTO for the enlightening discussion which makes this article becomes more readable.

REFERENCES

1. T. Haste, F. Payot, and P. D. W. Bottomley, "Transport and Deposition in the Phébus FP Circuit," *Annals of Nuclear Energy*. 2013. **61**:102–121.
2. L. Cantrel, F. Cousin, L. Bosland, K. Chevalier-Jabet, and C. Marchetto, "ASTEC V2 Severe Accident Integral Code: Fission Product Modelling and Validation," *Nuclear Engineering and Design*. 2014. **272**: 195–206.
3. G. Brilliant, C. Marchetto, and W. Plumecocq, "Fission Product Release from Nuclear Fuel II. Validation of ASTEC/ELSA on Analytical and Large-Scale Experiments," *Annals of Nuclear Energy*. 2013. **61**: 96–101.
4. L. Ammirabile, A. Bujan, and M. Sangiorgi, "PWR Medium Break LOCA Source Term Analysis using ASTEC Code," *Progress in Nuclear Energy*. 2015. **81**: 30–42.
5. D. L. Hanson, "Validation Status of Design Methods for Predicting Source Terms," *Nuclear Engineering and Design*. 2017. **329**: 60–72.
6. B. Ebiwonjumi, S. Choi, M. Lemaire, D. Lee, H. C. Shin, and H. S. Lee, "Verification and Validation of Radiation Source Term Capabilities in STREAM," *Annals of Nuclear Energy*. 2019. **124**: 80–87.
7. JAEA, "Fission Product Chemistry Database ECUME Version 1.1," Japan Atomic Energy Agency, Tokai-mura, 2019. doi: 10.11484/jaea-data-code-2019-017.
8. S. Nishioka, K. Nakajima, E. Suzuki, and M. Osaka, "An Experimental Investigation of Influencing Chemical Factors on Cs-chemisorption Behavior onto Stainless Steel," *Journal of Nuclear Science and Technology*. 2019. **00** (00):1–8.
9. K. Nakajima, S. Nishioka, E. Suzuki, and M. Osaka, "Study on Chemisorption Model of Cesium Hydroxide onto Stainless Steel Type 304," *International Conference on Nuclear Engineering, Proceedings, ICONE*, vol. 2019-May, 2019, doi: 10.1299/mej.19-00564.
10. F. G. Di Lemma, S. Yamashita, S. Miwa, K. Nakajima, and M. Osaka, "Prediction of Chemical Effects of Mo and B on the Cs Chemisorption onto Stainless Steel," *Energy Procedia*. 2017. **127**: 29–34.
11. M. Osaka *et al.*, "Results and Progress of Fundamental Research on Fission Product Chemistry - Progress Report in 2015," Japan Atomic Energy Agency, Tokai-mura, 2016. doi: 10.11484/jaea-review-2016-026.
12. F. Miradji, C. Suzuki, K. Nakajima, and M. Osaka, "Cesium Chemisorbed Species onto Stainless Steel Surfaces: An Atomistic Scale Study," *Journal of Physical and Chemistry of Solids*. 2018. **136**: 109168, 2020, doi: 10.1016/j.jpss.2019.109168.
13. C. Suzuki, K. Nakajima, and M. Osaka, "Phase Stability of Cs-Si-O and Cs-Si-Fe-O Compounds on Stainless Steel," *Journal of Nuclear Science and Technology*, pp. 1–12,

- Oct. 2021, doi: 10.1080/00223131.2021.1971576.
14. K. Nakajima, E. Suzuki, N. Miyahara, and M. Osaka, "An Experimental Investigation for Atmospheric effects on Cs Chemisorption onto Stainless Steel," *Progress in Nuclear Science and Technology*. 2018. **5** (0): 168–170.
 15. F. G. Di Lemma, K. Nakajima, S. Yamashita, and M. Osaka, "Surface Analyses of Cesium Hydroxide Chemisorbed onto Type 304 Stainless Steel," *Nuclear Engineering and Design*. 2016. **305**: 411–420.
 16. S. C. Jeon *et al.*, "A Comparative Study on the Cesium Retention Ability up to 1750 °C in Cs–Zr–Si–O, Cs–Al–Si–O, and Cs–Si–O," *Ceramics International*. 2019. **45** (12): 15754–15757.
 17. T. Minami *et al.*, "Structural Analysis of Alkali Cations in Mixed Alkali Silicate Glasses by ²³Na and ¹³³Cs MAS NMR," *Journal of Asian Ceramic Societies*. 2014. **2**(4): 333–338.
 18. S. Kaneko, Y. Tokuda, Y. Takahashi, H. Masai, and Y. Ueda, "Structural Analysis of Mixed Alkali Borosilicate Glasses Containing Cs + and Na + using Strong Magnetic Field Magic Angle Spinning Nuclear Magnetic resonance," *Journal of Asian Ceramic Societies*. 2017. **5**(1)7–12.
 19. E. Suzuki, K. Nakajima, M. Osaka, Y. Ohishi, H. Muta, and K. Kurosaki, "Low Temperature Heat Capacity of Cs₂Si₄O₉," *Journal of Nuclear Science and Technology*. 2020. **00** (00)1–6.